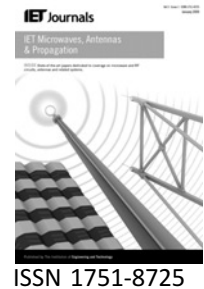


Published in IET Microwaves, Antennas & Propagation
 Received on 14th January 2008
 Revised on 13th November 2008
 doi: 10.1049/iet-map.2008.0008



Error performance of ultrawideband spatial multiplexing systems

J. Adeane¹ W.Q. Malik^{2,3} I.J. Wassell⁴

¹Fraser Research, 182 Nassau Street, Suite 301, Princeton, NJ 08542, USA

²Department of Brain and Cognitive Sciences, Massachusetts Institute of Technology, Cambridge, MA 02139, USA

³Massachusetts General Hospital, Harvard Medical School, Harvard University, Boston, MA 02114, USA

⁴Department of Engineering, University of Cambridge, Cambridge CB3 0FD, UK

E-mail: wqm@mit.edu

Abstract: In this paper, a number of ultrawideband (UWB) multiple-input multiple-output (MIMO) spatial multiplexing systems are presented and their error performance is analysed. For both model-based and measured UWB channels, the performance of various MIMO detectors is evaluated under the multiband orthogonal frequency division multiplexing (MB-OFDM) regime. Contrary to expectation, the results demonstrate that significant spatial diversity can be extracted, in addition to linear data-rate scaling, despite the large frequency diversity inherent in the UWB channel. It is shown that nonlinear detection schemes with reasonable complexity can provide considerable diversity gain, in contrast to well-known linear receivers. Thus, the proposed UWB spatial multiplexing schemes not only increase the data rate but also provide significant diversity gain and improved error rate performance.

1 Introduction

Ultrawideband (UWB) communication and localisation systems have attracted great interest during the last few years [1, 2]. UWB's novelty lies in its extremely wide bandwidth resulting in desirable capabilities such as accurate positioning and ranging and reduced small-scale fading. Various transmission schemes for UWB signalling have been proposed, including impulse radio and multiband orthogonal frequency division multiplexing (MB-OFDM). In this work, we adopt the MB-OFDM scheme, which has gained popularity for short range, very high data rate communications. MB-OFDM divides the available frequency band into several sub-bands, transmitting OFDM signals in different sub-bands at different times to achieve frequency and time diversity [3].

Spatially multiplexed multiple-input multiple-output (MIMO) systems increase the spectral efficiency dramatically by delivering high data rates without consuming additional power, bandwidth or time slots [4]. Based on multiple transmit and receive antennas and appropriate detection, the system effectively creates parallel MIMO subchannels to transmit independent streams of

data under the appropriate channel conditions. In this paper, we propose to combine MB-OFDM UWB with MIMO in order to improve both the throughput and reduce the error rates. Such a scheme is especially important for UWB applications that require very high data rates, as UWB systems cannot achieve a rate increase by simply boosting the transmit power, owing to regulatory limits [1]. In addition, some gain owing to spatial diversity may also be extracted, which can be critical to the operation of a UWB system that typically has a low pre-detection signal-to-noise ratio (SNR). Thus in Ref. [5], a multiple-antenna UWB system employing space-time coding (STC) demonstrated a considerable performance gain in terms of the bit-error rate (BER), contradicting the common perception that the frequency diversity inherent to UWB will saturate any diversity improvement. Although the scheme in Ref. [5] established the value of spatial processing for UWB error rate improvement, it did not directly provide any rate increase. The performance of a single-input multiple-output (SIMO) UWB impulse radio scheme was examined in Refs. [6] and [7]. It was found that increasing the number of receiving antennas provides extra diversity and is often more effective than increasing the number of rake receiver fingers. The setting of this

paper is different from the previous work, as we use the MB-OFDM approach instead of time-domain pulsed signalling, and also consider multiple transmit antennas as well as multiple receive antennas in a spatial multiplexing configuration. In this way, we obtain a large increase in the data rates as well as the potential for diversity gain.

In this paper, we extend the concept and techniques of MIMO spatial multiplexing to UWB systems, and evaluate the performance and complexity of some candidate detection techniques. To our knowledge, this is the first study that investigates MIMO spatial multiplexing in MB-OFDM UWB systems together with the implementation of some advanced detection schemes. Several authors have proposed the use of linear and maximum likelihood (ML) receiver in single-antenna UWB systems [3]. Linear receivers are simpler to implement than ML receivers; however, their performance falls far short of the optimum ML receiver. A number of other detectors, originally proposed for narrowband MIMO systems, offer substantially lower complexity. We are particularly interested in detectors that can exploit the potential of spatial diversity offered by the UWB channel. Thus, we evaluate the error-rate performance of a number of MIMO detectors via Monte-Carlo simulations using both measured and model-based statistical UWB channels.

2 System model

The UWB multipath channel is strongly frequency-selective and the channel-fading coefficients are therefore frequency-dependent. Following the discrete frequency domain matrix channel formulation in Ref. [8], the multiple-antenna UWB channel can be represented as, $\mathbf{H}^{(UWB)} \in \mathbb{C}^{N \times M \times F}$ where M , N and F denote the number of transmit antennas, receive antennas and frequency components, respectively. Here, $\mathbf{H}^{(UWB)}$ can be perceived as a frequency domain row vector, each of whose elements is the flat-channel MIMO matrix, $\mathbf{H}^{(f)}$, at frequency $f \in [f_l, f_h]$, where f_l and f_h define the lower- and upper-end frequencies of the channel transfer function. Note that in this discrete frequency domain representation, we assume that the frequency spacing of $\mathbf{H}^{(UWB)}$ is smaller than the coherence bandwidth, which is justified by the UWB channel measurement and modelling approaches considered.

Now introducing the concept of a multicarrier MIMO system, widely known as MIMO-OFDM, into our signal model, we can reduce the UWB channel into a set of F flat-fading channels, each centred at frequency f . Using this approach, for a given f , the $M \times N$ MIMO system can be written as

$$\mathbf{y}^{(f)} = \mathbf{H}^{(f)}\mathbf{x}^{(f)} + \mathbf{n}^{(f)} \quad (1)$$

where $\mathbf{x}^{(f)} = [x_1^{(f)}, x_2^{(f)}, \dots, x_M^{(f)}]$ and $\mathbf{y}^{(f)} = [y_1^{(f)}, y_2^{(f)}, \dots, y_N^{(f)}]$ are the transmitted and received signal vectors at f , respectively, $\mathbf{n}^{(f)} = [n_1^{(f)}, n_2^{(f)}, \dots, n_N^{(f)}]$ is the zero-mean complex additive Gaussian noise vector with unit

variance and $\mathbf{H}^{(f)}$ is the spatial channel matrix comprising the flat-fading coefficients. The channel matrix, $\mathbf{H}^{(f)}$, is normalised such that each underlying flat single-input single-output (SISO) channel has unit power. We will drop the superscript $(\cdot)^{(f)}$ in the subsequent discussion for notational convenience. Also note that in this spatial multiplexing system, x_m are the data bits originating from the m th transmit antenna, where $m = 1, \dots, M$. To make the comparison fair, we keep the total transmit power the same in all the cases considered.

At this time, the most widely accepted UWB channel model is based on the IEEE 802.15.3a standard, which specifies a modified Saleh-Valenzuela channel model [9]. The standard describes four typical indoor operating environments, referred to as channel models 1–4 (CM1–CM4) and is formulated for SISO systems. A naive way to extend it to MIMO is by using the model to generate $M \times N$ independent channels, ignoring the correlation between the spatial channels. As we will show later in this paper, this causes a discrepancy between the model-based channel simulation results and those obtained using the measured UWB channel owing to the effect of spatial correlation. To circumvent this inaccuracy, we propose the use of a fixed correlation model in our simulation [10]. Consequently, we introduce fixed transmit and receive correlation matrices, \mathbf{R}_{tx} and \mathbf{R}_{rx} , respectively, in accordance with the well-known Kronecker correlation model to yield

$$\mathbf{H} = \mathbf{R}_{rx}^{1/2} \mathbf{H}_w \mathbf{R}_{tx}^{1/2} \quad (2)$$

$$\mathbf{R}_{tx} = \begin{bmatrix} 1 & r_{12}^{tx} & \cdots & r_{1M}^{tx} \\ r_{12}^{tx*} & 1 & \ddots & \\ \vdots & & \ddots & r_{12}^{tx} \\ r_{1M}^{tx*} & r_{1M-1}^{tx*} & \cdots & 1 \end{bmatrix} \text{ and}$$

$$\mathbf{R}_{rx} = \begin{bmatrix} 1 & r_{12}^{rx} & \cdots & r_{1N}^{rx} \\ r_{12}^{rx*} & 1 & \ddots & \\ \vdots & & \ddots & r_{12}^{rx} \\ r_{1N}^{rx*} & r_{1N-1}^{rx*} & \cdots & 1 \end{bmatrix} \quad (3)$$

where $(\cdot)^*$ denotes the conjugate operation and \mathbf{H}_w is a stochastic $N \times M$ matrix given by the discrete Fourier transform (DFT) of the time domain UWB channel \mathbf{h}_w whose magnitude follows the Nakagami- m distribution. The method to generate \mathbf{h}_w is specified in the IEEE 802.15.3a standard [9]. Note that the dimensions of \mathbf{R}_{tx} and \mathbf{R}_{rx} are $M \times M$ and $N \times N$, respectively.

We now present some candidate receiver designs for spatially multiplexed UWB systems.

2.1 Traditional linear receiver

The linear receiver illustrated in Fig. 1 is the least complex detector. There are two well-known linear receivers, namely

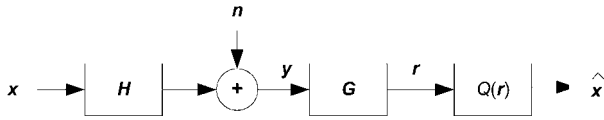


Figure 1 A simple representation of a linear receiver

zero forcing (ZF) and minimum mean square error (MMSE). Let us consider the received signal vector at frequency f . With linear receivers, \mathbf{y} is linearly transformed by a matrix equaliser \mathbf{G} as $\mathbf{r} = \mathbf{G}\mathbf{y}$, which is later quantised to obtain the symbol estimate, $\hat{x} = Q(\mathbf{r})$, where $Q(\cdot)$ denotes quantisation.

For the ZF receiver, the matrix equaliser is $\mathbf{G} = \mathbf{H}^\dagger$, where $(\cdot)^\dagger$ denotes the Moore–Penrose matrix pseudo-inverse. The ZF criterion suffers from noise enhancement, especially if the channel matrix \mathbf{H} is rank-deficient or ill-conditioned. For the MMSE receiver, the matrix equaliser

$$\mathbf{G} = \sigma^2 \mathbf{H}^H (\sigma^2 \mathbf{H} \mathbf{H}^H + \sigma_n^2 \mathbf{I}_M)^{-1} \quad (4)$$

minimises the error as a result of both noise and interference, where σ^2 is the signal power and σ_n^2 is the noise power. Note that the SNR per dimension (i.e. per antenna and per subcarrier) in UWB systems is very low; therefore ZF may experience high error rates owing to noise enhancement.

There are some nonlinear MIMO detection techniques that perform better than linear receivers and yet have only moderately high complexity. The lower bound for the BER is given by the performance of the ML detector, which also has the highest complexity that increases exponentially with the channel dimensionality.

2.2 V-BLAST receiver

In their pioneering work, Golden *et al.* [11] provided a multi-antenna prototype that achieves very high spectral efficiency using the V-BLAST detection algorithm, realising a good tradeoff between complexity and performance. V-BLAST detection employs an ordered serial nulling plus cancellation technique. Note that the nulling process can be performed by using the ZF or MMSE criteria; in this paper, we refer to these two schemes as ZF-VBLAST and MMSE-VBLAST. The optimum detection order is determined such that the minimum post-detection SNR of all data streams is maximised, and is from the strongest to the weakest signal in such a strategy. In this work, we extend the narrowband V-BLAST detection algorithm in Ref. [11] to MB-OFDM UWB systems.

2.3 Partial decision feedback receiver

In Ref. [12], Waters and Barry proposed a partial decision-feedback (PDF) detector, which is a combination of ordered decision-feedback (ODF) detector and the linear detector, applicable to MIMO systems. This combination is necessary because the ODF detector requires an order of

magnitude more computations than the linear detectors. However, it should be noted that the ODF can significantly outperform a linear detector, provided that the signals are detected using BLAST ordering [12]. Using a low-complexity implementation, PDF was shown to require only 38% of the computation required for V-BLAST. An important advantage of ODF and PDF detectors (which are based on noise prediction) is that they only require knowledge of the noise autocorrelation matrix, and not the channel. In this paper, we extend the PDF algorithm proposed in Ref. [12] to UWB systems. Referring to Fig. 1, PDF detection begins with linear detection, and in the case of the ZF criterion the equalised signal can be written as

$$\mathbf{r} = \mathbf{G}\mathbf{y} = \mathbf{G}\mathbf{H}\mathbf{x} + \mathbf{G}\mathbf{n} \quad (5)$$

where $\mathbf{G} = \mathbf{H}^\dagger$. Now, (3) can be rewritten as

$$\mathbf{r} = \mathbf{x} + \mathbf{w},$$

where $\mathbf{r} = [r_1, r_2, \dots, r_M]$ and the noise $\mathbf{w} = [w_1, w_2, \dots, w_M]$ has autocorrelation matrix $E[\mathbf{w}\mathbf{w}^H] = \sigma_w^2 (\mathbf{H}^H \mathbf{H})^{-1}$. Note that here σ_w^2 is the noise variance after the equaliser. Based upon the output of the linear detector, we detect and quantise the symbol with the smallest MSE. It can be shown that the MSE of the first symbol is proportional to the squared norm of the corresponding row of the channel pseudo-inverse and therefore, the index of the first detected symbol is [12]

$$i_1 = \arg \min \|\mathbf{g}_j\|^2, \quad j \in \{1, \dots, N\} \quad (6)$$

where \mathbf{g}_j is the j th row of \mathbf{G} . The first detected symbol that has the smallest MSE, \hat{x}_{i_1} , is found by quantising \hat{r}_{i_1} directly. For the other symbols, the PDF detector applies linear prediction to reduce the noise variance before quantising. Note that based upon the detection of the symbol having the smallest MSE, \hat{x}_{i_1} , the receiver deduces the i_1 th noise sample

$$\mathbf{w}_{i_1} = \mathbf{r}_{i_1} - \mathbf{x}_{i_1} \quad (7)$$

Based on the correlation between noise samples, we can exploit the knowledge of \mathbf{w}_{i_1} and predict \mathbf{w}_{i_v} for $v > 1$. Let $q_v (r_{i_1} - \hat{x}_{i_1})$ denote the predicted value of \mathbf{w}_{i_v} based on \mathbf{w}_{i_1} for some constants q_v . The PDF detector subtracts this predicted noise sample from \mathbf{r}_{i_v} , and therefore when the symbol with the smallest MSE is detected correctly, the noise variance for the i_v th symbol is reduced to [12]

$$\begin{aligned} E[\|\mathbf{w}_{i_v} - q_v \mathbf{w}_{i_1}\|^2] &= E[\|\mathbf{g}_{i_v} \mathbf{n} - q_v \mathbf{g}_{i_1} \mathbf{n}\|^2] \\ &= \sigma_n^2 \|\mathbf{g}_{i_v} - q_v \mathbf{g}_{i_1}\|^2 \end{aligned} \quad (8)$$

When q_v is chosen to minimise the noise variance, the term $q_v \mathbf{g}_{i_1}$ reduces to the projection of \mathbf{g}_{i_v} onto the subspace spanned by \mathbf{g}_{i_1} and this leads to a simple equation for

finding the prediction coefficients [10]

$$q_v = \mathbf{g}_{i_v} \mathbf{g}_{i_1}^H \|\mathbf{g}_{i_1}\|^2 \quad (9)$$

Once the prediction coefficients have been calculated they are used to implement the noise predictor. The v th symbol is detected according to

$$\hat{x}_{i_v} = Q\{y_{i_v} - q_v(y_{i_1} - \hat{x}_{i_1})\}. \quad (10)$$

2.4 ML receiver

The ML receiver is known to yield the best BER performance. However, its computational complexity grows exponentially with the transmit antenna array size. The complexity is prohibitive for higher-order constellations or when the number of transmit dimensions is large. Consequently, for a system such as UWB, which has a large number of subcarriers, ML detection is impractical. However, we include the analysis of the ML receiver extended to the UWB spatial multiplexing regime as a benchmark for receiver performance.

3 Performance analysis

The diversity available to a wireless system is characterised by the number of independently fading branches, which is also referred to as the diversity order. For a given SNR, let $R(\text{SNR})$ be the transmission rate and $P_e(\text{SNR})$ be the corresponding error probability. The diversity gain and multiplexing gain are defined as [13]

$$\text{Diversity gain} = - \lim_{\text{SNR} \rightarrow \infty} \log \frac{P_e(\text{SNR})}{\log(\text{SNR})}$$

$$\text{Multiplexing gain} = - \lim_{\text{SNR} \rightarrow \infty} \log \frac{R(\text{SNR})}{\log(\text{SNR})}$$

In this section, we will investigate the diversity and spatial multiplexing gain that the proposed MIMO spatial multiplexing system can achieve with an appropriate receiver. It is worth emphasising that the data rates achieved by each of these MIMO-OFDM UWB systems is proportional to the number of transmit antennas. Therefore depending on the choice of detector, we can scale up the data rate compared with the SISO case while also improving the BER performance.

Although both diversity and coding improve the system performance by decreasing the error rate, the manifestation of these gains is very different. The diversity gain translates to an increase in the slope of the BER curve, whereas the coding gain shifts the error rate curve to the left. The SNR advantage as a result of diversity gain increases at higher diversity order and lower target error rate. On the other hand, the coding gain is typically constant at high enough SNR. In this paper, an uncoded system is considered as we are interested in the diversity and rate improvement to UWB systems owing to multiple antennas.

3.1 Channel description and measurement setup

The performance of the detectors described previously is now evaluated via Monte-Carlo simulation for the UWB channels as described in Section 2. The channel realisations are obtained from measurements and also generated from appropriately modified models based on the current UWB standards.

In this paper, we concentrate on the indoor, short-range line-of-sight (LOS) environment, as this is likely to be a common scenario in a small office or home environment, especially for commonly perceived applications such as wireless USB. This scenario is referred to as CM1 in Ref. [9]. As the preliminary models in Ref. [9] are mainly intended to allow a fair comparison between the various system proposals submitted to the standardisation bodies, our analysis is complemented with results obtained using practical channel measurements conducted in an indoor MIMO setting. The details of the UWB channel measurement procedure can be found in Ref. [8].

3.2 Simulation results

The simulation results presented in this section are based on 2×2 and 3×3 spatial MIMO arrays, QPSK modulation, uncoded transmission and the UWB channels described previously. The cyclic prefix is longer than the length of the multipath channel to avoid inter-symbol interference (ISI). We do not implement time-frequency interleaving.

Figs. 2 and 3 show the performance results for $M = N = 2$, for systems operating in the model-based and measured UWB channels, respectively. In both figures, it can be seen that the VBLAST receivers outperform the linear receivers. For the 2×2 and 3×3 systems in Figs. 2 and 4, respectively, MMSE-VBLAST outperforms MMSE by 7 dB and 11 dB, respectively at $\text{BER} = 10^{-3}$. The linear receivers achieve a diversity order of 1 in both 2×2 and 3×3 configurations, whereas the MMSE-VBLAST receiver achieves a higher diversity order especially as the number of antennas increases. These observations extend previously presented results concerning diversity order for linear and nonlinear detectors in narrowband MIMO systems [4].

The BER curves tend to spread out as N increases, as nonlinear receivers are able to utilise the greater diversity offered by the use of more receiver antennas. Also, the performance curves of the linear receivers in the symmetrical array configuration (Figs. 2 and 4) degrade as the number of transmit and receive antennas increases. The reason is the increased multistream interference (MSI), which dominates the additive Gaussian noise. As an ZF receiver suffers greater noise enhancement than an MMSE receiver, the latter is expected to perform better at larger array sizes.

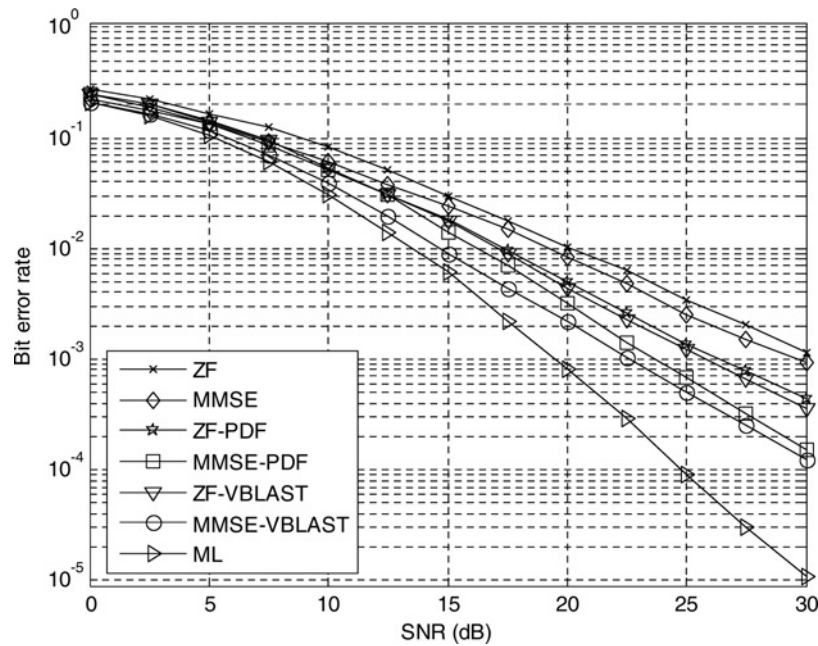


Figure 2 BER performance of 2×2 MIMO-UWB systems for various detection algorithms based on the indoor channel simulation model CM1

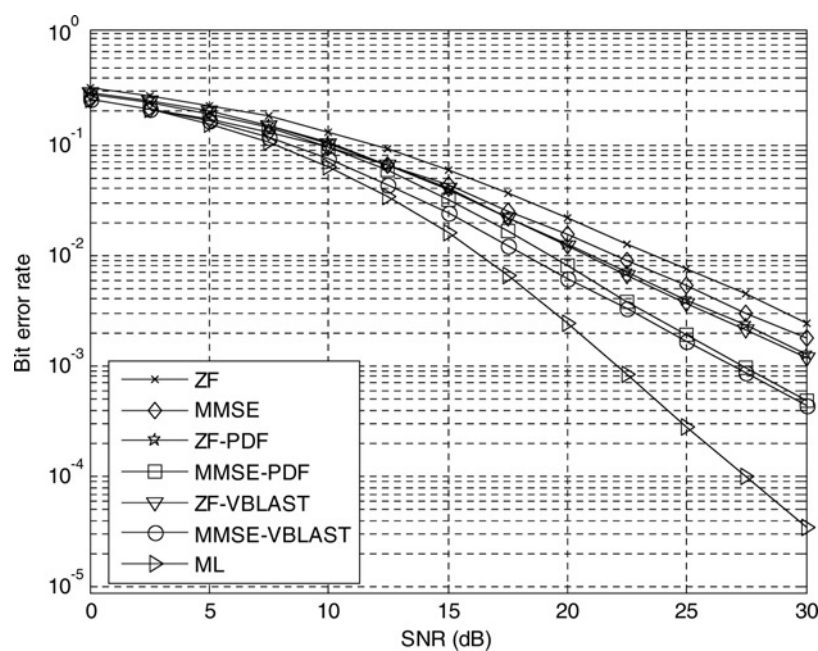


Figure 3 BER performance of 2×2 MIMO-UWB systems for various detection algorithms for the indoor channel based on measurements

Figs. 4 and 5 show the performance results for $M = N = 3$ in the model-based and measured channels, respectively. A comparison of the respective 2×2 and 3×3 performance curves reveals that the linear receivers fail to take advantage of the additional diversity available. On the other hand, MMSE-VBLAST and ML offer further performance improvements as the number of antennas increases, which can be seen from the steeper slope of the BER curves at high SNR.

The results using measured channels agree closely with the trends observed with the model-based channels, demonstrating the robustness of our proposed receivers. However, a shift in the BER curves of model-based and measured channels is apparent. This is to be expected, as the UWB channel simulation, in which each subchannel is modelled independently, does not take into account the finite correlation between the MIMO branches. Note that some non-zero correlation will usually exist in the measured

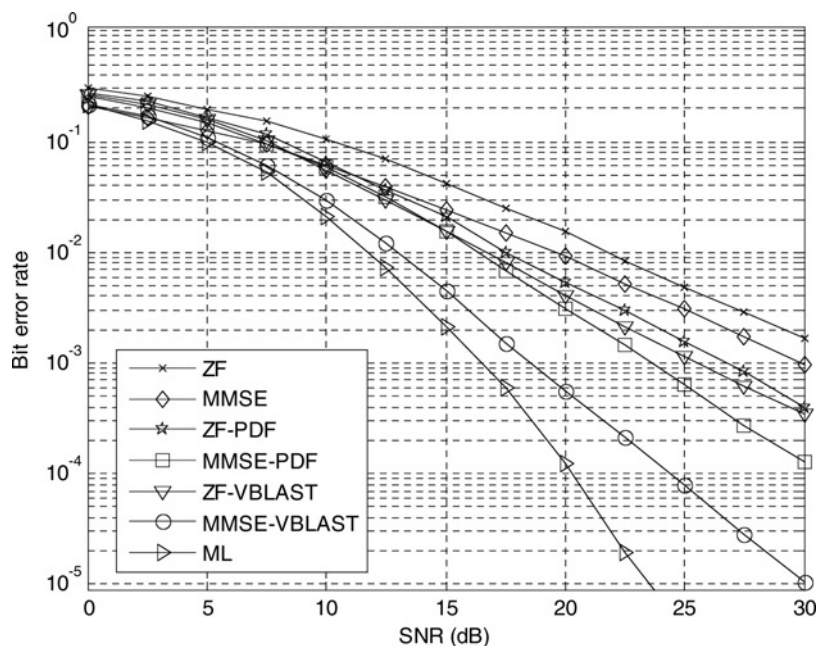


Figure 4 BER performance of 3×3 MIMO-UWB systems for various detection algorithms based on the indoor channel simulation model CM1

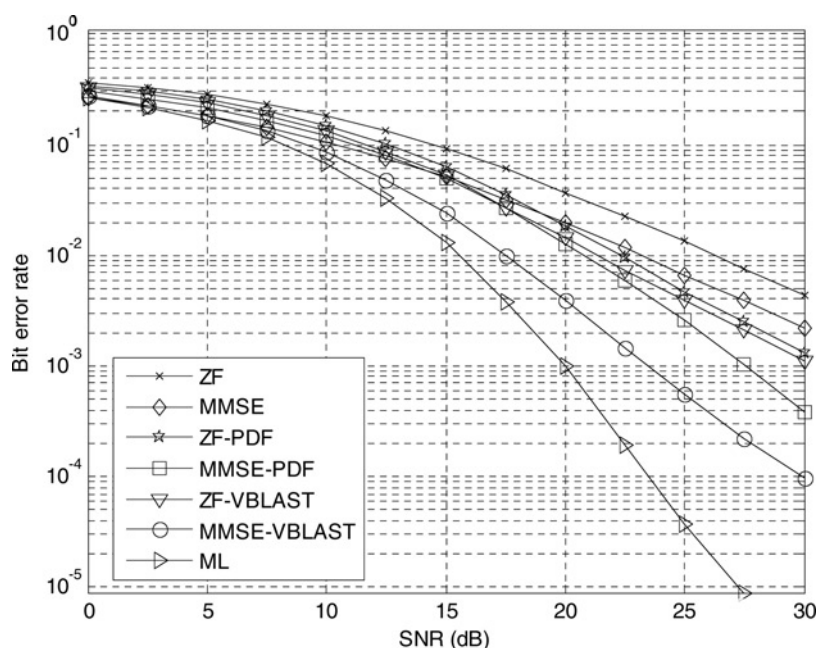


Figure 5 BER performance of 3×3 MIMO-UWB systems for various detection algorithms for the indoor channel based on measurements

channels, although on average it is well below 0.5 for the antenna separation used in Ref. [8]. Therefore the results in Figs. 2 and 4 for the UWB channel simulation model yield a somewhat optimistic estimate of the system performance, as this channel model neglects the effect of the residual correlation encountered in an actual MIMO environment. Using the fixed correlation model that we proposed in Ref. [13], Fig. 6 shows that with the antenna correlation value set to 0.45, the results for the simulated and measured channels agree closely for the MMSE

receiver in a 2×2 system. Nevertheless, our interest here lies in the relative performance of the various detectors rather than the absolute performance levels. It can be seen from Figs. 2–5 that the results based on channel measurements show the same trends in terms of relative detector performance as compared with those based on the modified IEEE channels.

Using the ML detector as a baseline comparison, Fig. 7 shows the advantage of multiple antennas in increasing the

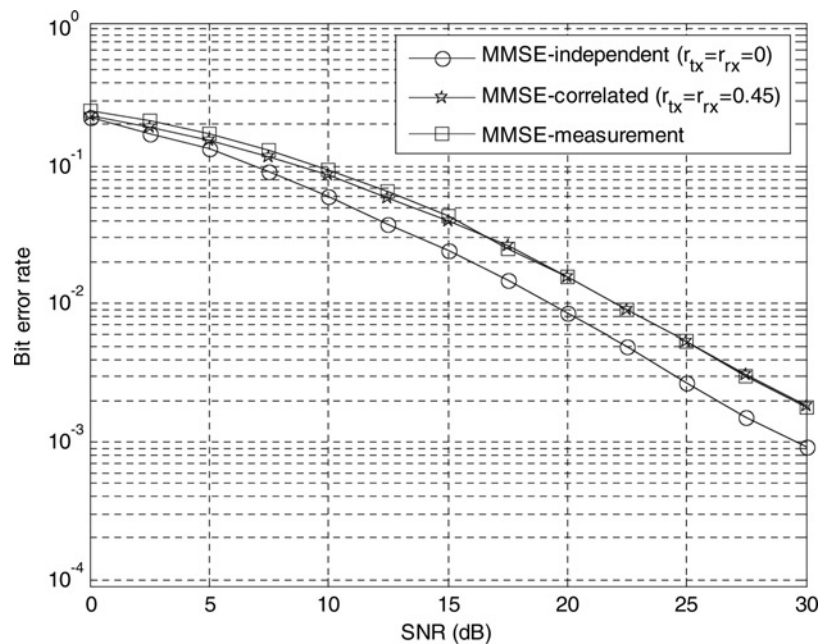


Figure 6 BER performances of 2×2 MIMO UWB systems with a MMSE receiver for a simulated channel model having various correlation values and for a measurement-based channel

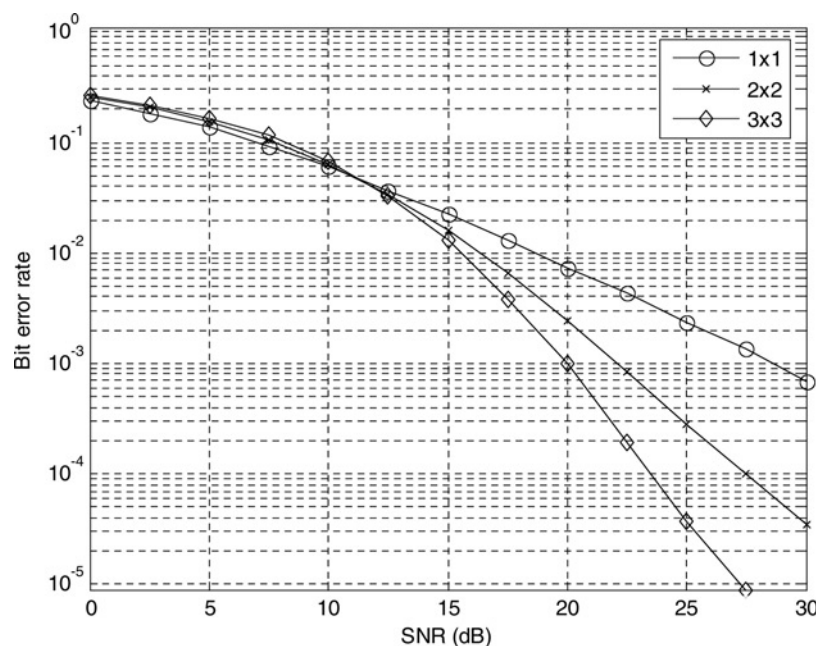


Figure 7 BER performance of an ML receiver for the symmetrical (i.e. $M \times N$, $M = N$) MIMO array structure for an indoor channel based on measurements, with $M = 1, 2, 3$

data rate and reducing the error rate in UWB systems. From Figs. 7 and 8, we can see that the diversity order increases with the number of receiver antennas both with symmetrical and asymmetrical array structures. Increasing the number of transmit antennas will increase the data rate, although not necessarily the BER performance, as we can see by comparing Figs. 7 and 8. The slopes of the curves show that a 3×3 MIMO array with an ML detector provides similar diversity performance as a 1×3 array. The former, of course, also provides a 3-fold rate increase compared with the latter.

We observe that the performance of uncoded spatial multiplexing UWB systems is almost identical for all of the IEEE 802.15.3a channel scenarios, namely CM1–CM4. This finding is confirmed by the results of simulations conducted using our measurement-based channels in LOS and non-line-of-sight scenarios. Similar behaviour was reported in the context of uncoded multiband SISO and MIMO UWB with space-time-frequency coding but without channel coding in Ref. [14]. It was proven theoretically that the performance and diversity gain of uncoded MB-OFDM

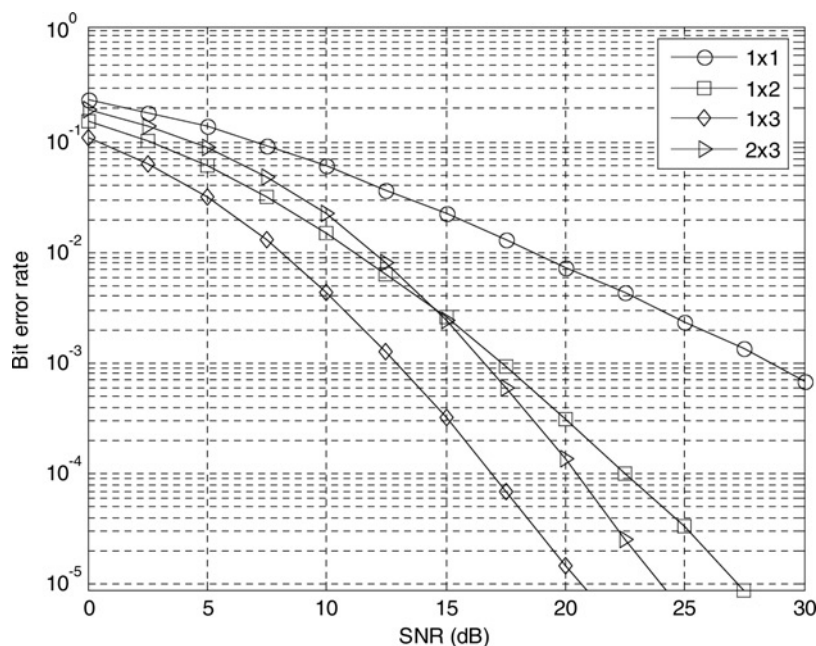


Figure 8 BER performance of an ML receiver for asymmetrical (i.e. $M \times N$, with $M \neq N$) MIMO array structure for an indoor channel based on measurements

UWB systems is not affected by the clustered multipath arrivals observed in channel scenarios CM1–CM4.

3.3 Receiver complexity

We now discuss and compare the computational complexity of the various UWB spatial multiplexing detection schemes, which is important for practical implementation. Under OFDM, the UWB channel is divided into a set of F flat-fading or narrowband channels, and the detection process is performed separately at each subcarrier. Table 1 lists the number of arithmetic operations required for a narrowband detector, where Q is the QAM constellation order [15]. Also shown is the number of operations for the corresponding UWB system comprising F narrowband subcarriers.

As an example, for a 16-QAM UWB-OFDM system with 64 carriers, 4 transmit and 4 receiver antennas, the number of arithmetic operations required for the linear, V-BLAST and ML detectors is 1792, 2816 and 16384, respectively. Clearly the ML detector is unrealistic for implementation in practical systems, necessitating the need

Table 1 The computational complexity of various UWB spatial multiplexing reception schemes

Detector	Number of arithmetic operations	
	Narrowband	UWB
linear detector	$M(2N - 1)$	$FM(2N - 1)$
V-BLAST	$M(3N - 1)$	$FM(3N - 1)$
ML (exhaustive search)	$Q^{M/2}$	$FQ^{M/2}$

to consider the alternatives, some of which have been discussed and compared in this paper.

4 Conclusion

In this paper, we have extended narrowband MIMO spatial multiplexing schemes to the MB-OFDM UWB regime. Similar to the results in narrowband systems, it is found that suboptimum nonlinear detection techniques significantly outperform linear receivers. Our results establish that with an appropriate detection scheme, an increasing number of antennas not only yield a higher data rate but also a significantly improved diversity order. We have analysed the use of several detection methods, each of which offers a different performance complexity tradeoff. For example, the PDF receiver is less complex than V-BLAST; however, MMSE V-BLAST offers better performance especially as the number of antennas is increased. Our analysis suggests the existence of some residual spatial correlation between the MIMO subchannels in practical situations. The BER performance can be severely degraded by channel correlation and therefore it is important to take spatial correlation into account in UWB system design and performance evaluation. This effect can be well approximated using a fixed correlation model, which gives results that closely match those obtained from measurements.

5 References

- [1] ALLEN B., DOHLER M., OKON E.E., MALIK W.Q., BROWN A.K., EDWARDS D.J. (EDS.): 'Ultra-wideband antennas and propagation for communications, radar and imaging' (Wiley, London, UK, 2006)

- [2] ROY S., FOERSTER J.R., SOMAYAZULU V.S., LEEPER D.G.: 'Ultrawideband radio design: the promise of high-speed, short-range wireless connectivity', *Proc. IEEE*, 2004, **92**, (2), pp. 295–311
- [3] BATRA A., BALAKRISHNAN J., DABAK A., GHARPUREY R., LIN J., FONTAINE P., HO J.-M., LEE S., FRECHETTE M., MARCH S., YAMAGUCHI H.: 'Multiband OFDM physical layer proposal for IEEE 802.15 Task Group 3a', IEEE P802.15-03/268r0-TG3a, July 2003
- [4] PAULRAJ A.J., NABAR R., GORE D.: 'Introduction to space-time wireless communications' (Cambridge University Press, Cambridge, UK, 2003)
- [5] YANG L., GIANNAKI G.B.: 'Analog space-time coding for multiantenna ultra-wideband transmissions', *IEEE Trans. Commun.*, 2004, **52**, (3), pp. 507–517
- [6] MALIK W.Q., EDWARDS D.J.: 'UWB impulse radio with triple polarization SIMO'. Proc. IEEE Globecom, Washington, DC, USA, November 2007, pp. 4124–4128
- [7] KEIGNART J., ABOU-RJEILY C., DELAVEAUD C., DANIELE N.: 'UWB SIMO channel measurements and simulations', *IEEE Trans. Microw. Theory Techn.*, 2006, **54**, (4), pp. 1812–1819
- [8] MALIK W.Q., EDWARDS D.J.: 'Measured MIMO capacity and diversity gain with spatial and polar arrays in ultrawideband channels', *IEEE Trans. Commun.*, 2007, **55**, (12), pp. 2361–2370
- [9] MOLISCH A.F., FOERSTER J.R., PENDERGRASS M.: 'Channel models for ultrawideband personal area networks', *IEEE Wireless Commun.*, 2003, **10**, (6), pp. 14–21
- [10] ADEANE J., MALIK W.Q., WASSELL I.J., EDWARDS D.J.: 'A simple correlated channel model for ultrawideband MIMO systems', *IET Microw., Antenna, Propag.*, 2007, **1**, (6), pp. 1177–1181
- [11] GOLDEN G.D., FOSCHINI G.J., VALENZUELA R., WOLNIANSKY P.W.: 'Detection algorithm and initial laboratory results using the V-BLAST space-time communication architecture', *Electron. Lett.*, 1999, **35**, (1), pp. 14–16
- [12] WATERS D.W., BARRY J.R.: 'Partial decision-feedback detection for multiple-input multiple-output channels'. Proc. IEEE ICC 2004, Paris, France, June 2004
- [13] ZHENG L., TSE D.N.C.: 'Diversity and multiplexing: a fundamental tradeoff in multiple-antenna channels', *IEEE Trans. Inform. Theory*, 2003, **49**, (5), pp. 1073–1096
- [14] SIRIWONGPAIRAT W.P., SU W., RAY LIU K.J.R.: 'Performance characterization of multiband UWB communication systems using Poisson cluster arriving fading paths', *IEEE J. Select. Areas Commun.*, 2006, **24**, (4), pp. 745–751
- [15] WINDPASSINGER C., LAMPE L., FISCHER R.F.H., HEHN T.: 'A performance study of MIMO detectors', *IEEE Trans. Wireless Commun.*, 2006, **5**, (8), pp. 2004–2008